Materials Science & Engineering A 777 (2020) 139074

Contents lists available at ScienceDirect

Materials Science & Engineering A

journal homepage: http://www.elsevier.com/locate/msea

Short communication

Tuning heterostructures with powder metallurgy for high synergistic strengthening and hetero-deformation induced hardening

Z.K. Li [a], X.T. Fang [c], Y.F. Wang [b], P. Jiang [d], J.J. Wang [a,*], C.M. Liu [a], X.L. Wu [d], Y.T. Zhu [c,e,**], C. C. Koch [c]

[a] Key Laboratory for Anisotropy and Texture of Materials of Ministry of Education, Northeastern University, Shenyang, 110819, People's Republic of China
[b] The State Key Laboratory of Rolling and Automation, Northeastern University, Shenyang 110819, China
[c] Department of Materials Science and Engineering, North Carolina State University, Raleigh, NC, 27695, USA
[d] State Key Laboratory of Nonlinear Mechanics, Institute of Mechanics, Chinese Academy of Science, Beijing, 100190, People's Republic of China
[e] Nano and Heterogeneous Materials Center, School of Materials Science and Engineering, Nanjing University of Science and Technology, Nanjing, 210094, People's Republic of China

ARTICLE INFO

Keywords:
Heterogeneous lamella structure
Synergistic strengthening
Hetero-deformation induced hardening
Powder metallurgy

ABSTRACT

Heterogeneous-lamella-structured Fe-Cu composites were fabricated using powder metallurgy, displaying an inverse "banana" curve between the strength and ductility. The density of domain interfaces and the strength difference between hard and soft domains can be tuned independently, providing a promising way to further study the hetero-deformation induced strengthening mechanisms of heterogeneous-lamella-structures.

1. Introduction

Heterostructured (HS) materials, defined as materials containing domains with dramatic strength difference [1], have attracted extensive attention in the materials community, due to their superior combination of strength and ductility. Several groups of materials are considered as HS materials, including materials with gradient structure [2–4], harmonic structure [5,6], heterogeneous lamella structure (HLS) [7,8], bimodal structure [9,10], dual-phase structure [11,12] and laminate structure [13–15]. Among these heterostructures, HLS is considered as the near-ideal structure for superior mechanical performance and has potential for large-scale engineering applications [1].

The fundamental physics that renders HLS materials superior mechanical performance is their ability in producing synergistic strengthening induced by hetero-deformation induced (HDI) stress and extra strain hardening (HDI hardening) [16,17], both of which are highly dependent on the heterostructure. It is the heterostructure that leads to the hetero-deformation, producing HDI stress near the domain interface, which produces the synergistic strengthening and the HDI hardening. There are three main heterostructural parameters that significantly affect the synergistic strengthening and HDI hardening, and consequently affect the mechanical performance of HLS materials. They are density of domain interfaces, strength difference between hard and soft domains and the geometries of soft domains. Thus, to further study the hetero-deformation induced strengthening mechanisms of HLS materials and to optimize their mechanical performance for engineering applications, it is critical to tune HLSs with these three aspects. However, so far, HLSs are formed during annealing through partial recrystallization or through phase transformation [7,8]. The formation of HLSs is sensitive to the plastic deformation before annealing and to the annealing conditions. The amount and the geometries of as-formed soft domains, as well as the strength difference between hard and soft domains, are always associated with each other and change simultaneously during annealing, making it very difficult to independently tune these heterostructural parameters. Thus, new approaches for fabricating HLS materials need to be explored to tune the heterostructure.

Powder metallurgy is a mature materials processing technique that can be easily utilized in the laboratory or at industrial scale. With the development of sintering techniques, various metallic materials, including alloys, metallic glass and nanocrystalline metallic materials, have been successfully fabricated by powder metallurgy [18–21]. Logically, it should be a promising technique for fabricating HLS materials. In this paper, we present a new strategy to produce HLS materials using powder metallurgy and subsequent thermal-mechanical processes.

* Corresponding author.
** Corresponding author. Department of Materials Science and Engineering, North Carolina State University, Raleigh, NC, 27695, USA.
E-mail addresses: wangjj@smm.neu.edu.cn (J.J. Wang), ytzhu@ncsu.edu (Y.T. Zhu).

https://doi.org/10.1016/j.msea.2020.139074
Received 5 December 2019; Received in revised form 8 January 2020; Accepted 5 February 2020
Available online 8 February 2020

The as-produced HLS Fe-Cu composites possess a superior combination of strength and ductility (an inverse banana curve), as compared with the pure iron counterpart. Moreover, the density of Fe-Cu domain interfaces was tuned independently without affecting the strength difference between hard iron and soft copper domains.

2. Experimental procedure

Commercial copper (99.9 wt%) and iron (99.9 + wt%) powder were mixed with three volume fractions of copper powder (15%, 30% and 40%) and were compacted into $\Phi 10 \times 1.2$ mm disks under 4 GPa for 1 min. The disks were sintered at 1050 °C for 2 h under a reducing atmosphere (95% Nitrogen and 5% Hydrogen) in a tube furnace and were cooled down first to 600 °C with a cooling rate of 2 °C/min and then to ambient temperature with the furnace. Before cold rolling, the as-sintered disks were mechanically polished to a near-mirror finish. A total thickness reduction of ~81% (from 1.1 mm to 0.2 mm) was achieved after multi-pass cold rolling, and in each pass the reduction was ~0.1 mm. As-rolled plates were finally annealed at 360 °C for 30 min. Pure iron samples made of the same iron powder were also produced with the same procedure for comparison. Microstructures were characterized by using a Zeiss optical microscope and an FEI Quanta 3D FEG instrument with Ion Channeling Contrast Microscopy (ICCM) and electron backscatter diffraction (EBSD). Vickers hardness was measured by a Mitutoyo hardness tester (HM112). Dog-bone shaped samples with gauge dimensions of $0.2 \times 2.5 \times 10$ mm^3 were cut from the center of the as-annealed plates for uniaxial tension and loading-unloading-reloading (LUR) tests.

3. Results and discussion

In the following, HLS Fe-Cu samples with *x*% (vol.) copper volume fraction are labeled as Fe-*x*Cu, including Fe-15Cu, Fe-30Cu and Fe-40Cu. Fig. 1a–c shows the cross-sectional optical micrographs of Fe-15Cu, Fe-30Cu and Fe-40Cu samples. The color contrast clearly indicates that elongated copper domains are embedded in iron matrix along the rolling direction. With more copper powder added, the density of Fe-Cu domain interfaces becomes larger. It should be noticed that, due to the clustering of copper domains, the density of Fe-Cu domain interfaces does not increase linearly with increasing the volume fraction of copper powder. The Vickers hardness results (Fig. 1d) reveal that the hardness of both iron and copper domains almost remains unchanged in all three HLS Fe-Cu composites, indicating that the strength difference between hard iron and soft copper domains stays the same. The hardness of iron domains in HLS Fe-Cu samples is slightly higher than the hardness of pure iron samples, which is caused by the strengthening induced by copper precipitation [22,23].

Fig. 2a–c are ICCM images (along the rolling surface) showing microstructures of HLS Fe-Cu samples. In all Fe-Cu samples, the iron domains are coarse-grained, while the copper domains are fine-grained with an average grain size of about 1 μm. These microstructural images support the hardness results shown in Fig. 1d, suggesting that the mechanical properties of iron and copper domains do not change with increasing copper contents. In the magnified EBSD image (Fig. 2d), sharp and void-free Fe-Cu interfaces are shown between iron and copper domains, indicating a good sintering finish. Iron precipitation can be found at copper grain boundaries, which hinders the grain growth of copper, keeping the grain size around 1 μm after annealing at 360 °C. Several iron-rich zones at copper grain boundaries are circled in Fig. 2d. Likewise, there are also some copper precipitates near the grain boundaries in iron domains.

Fig. 3a shows the engineering strain-stress curves of pure iron samples and HLS Fe-Cu samples. As shown, the pure iron sample (with a uniform elongation ~1.4%) starts necking soon after yielding at 580 MPa. To estimate the mechanical properties of iron domains in HLS Fe-Cu samples, the pure iron samples were processed the same way as the HLS samples. And the precipitation of copper in iron domains, which approximately leads to a strength increment of 60 MPa, based on the Vickers hardness results, has negative impact on the ductility [22]. Therefore, the yield strength and the uniform elongation of iron domains in HLS Fe-Cu samples can be estimated as ~640 MPa and less than 1.4% respectively. The yield strength and the uniform elongation of copper domains are estimated as ~260 MPa and ~12% respectively, based on their grain sizes [24,25]. Although the precipitation of iron also

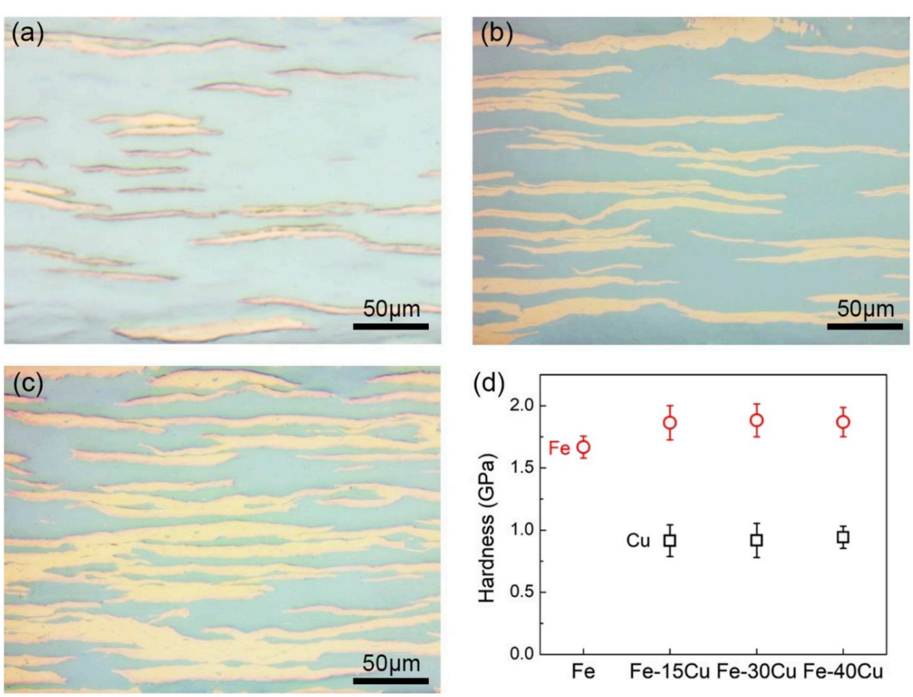

Fig. 1. (a–c) Optical micrographs (cross-sectional view) for Fe-15Cu, Fe-30Cu and Fe-40Cu heterogeneous-lamella-structured samples, respectively; (d) Vickers microhardness measured on pure iron samples and the Fe and Cu domains, using a load of 10 g.

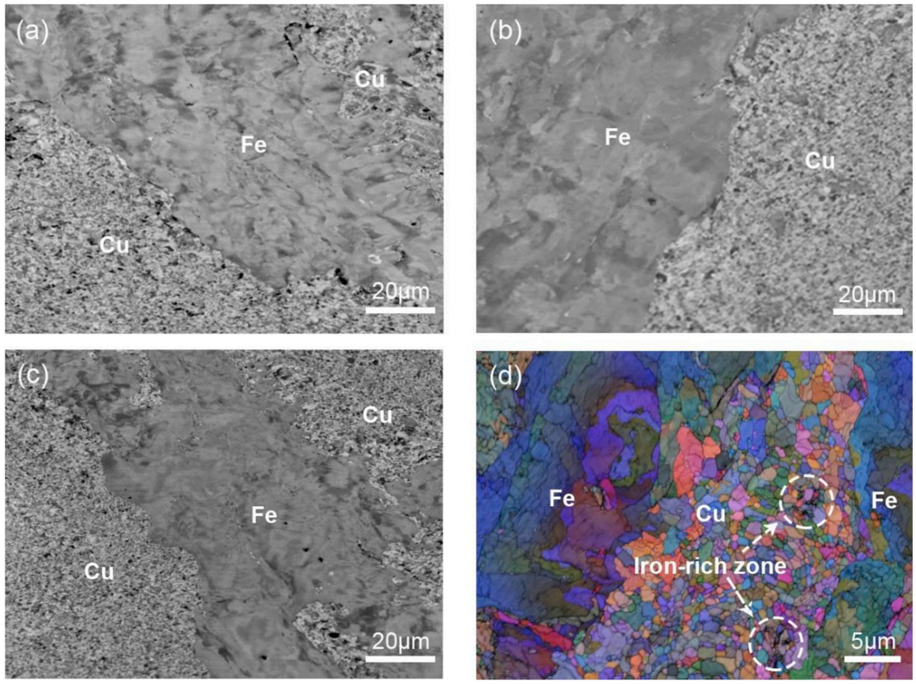

Fig. 2. (a), (b) and (c) ICCM images of as-processed Fe-15Cu, Fe-30Cu and Fe-40Cu samples. (d) EBSD observation of the iron/copper interface in Fe-40Cu sample.

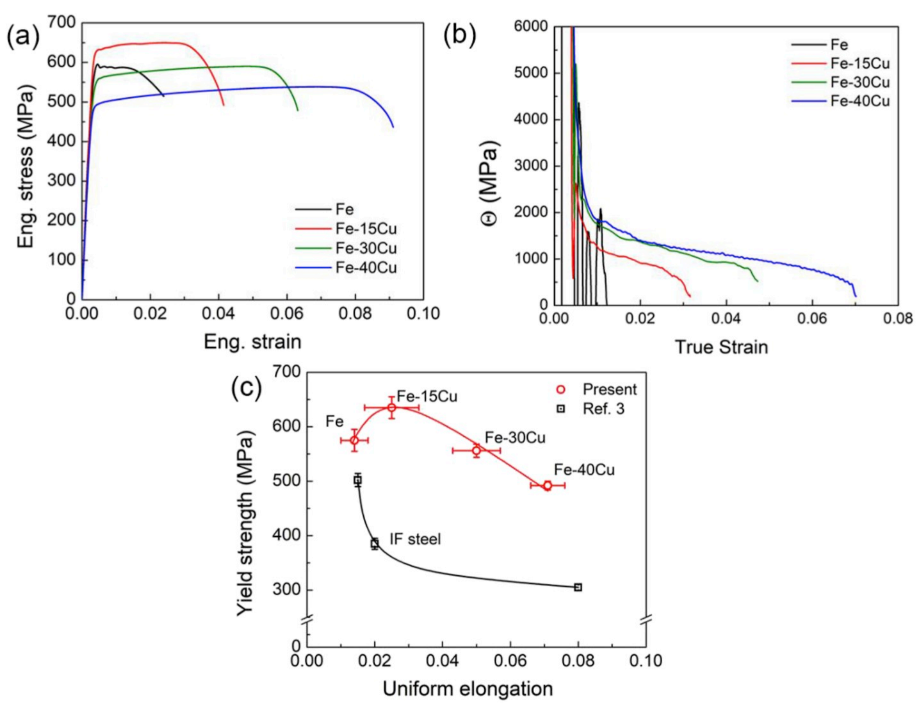

Fig. 3. (a) and (b) Engineering strain-stress curves and strain hardening curves of pure iron and Fe-15Cu, Fe-30Cu and Fe-40Cu HLS samples. (c) Comparison of the strength and ductility between Fe-Cu HSL samples and homogeneous IF steel samples [4].

strengthens copper domains, its impact on the global strength is negligible, as copper domains are soft domains in the HLS materials.

Compared with the above estimated mechanical properties of individual iron and copper domains, it is obvious that HLS Fe-Cu samples possess superior combination of strength and ductility, as shown in Fig. 3a. The advantage in mechanical performance of HLS Fe-Cu samples is further demonstrated by a comparison with the strength-ductility relationship of homogeneous IF steels [4]. As shown in Fig. 3c, the IF steel exhibits a typical banana curve with a significant tradeoff between strength and ductility, while the HLS Fe-Cu composites show an inversed banana curve. The outstanding combination of strength and ductility is attributed to synergistic strengthening and HDI hardening. During deformation of HLS Fe-Cu samples, soft copper domains first start yielding, while hard iron domains remain elastic. This is a hetero-deformation scenario where copper domains accommodate more strain than iron domains. A plastic strain gradient is then produced in the soft copper domain near the Fe-Cu domain interface, as the strain needs to be continuous among iron and copper domains. The plastic strain gradient is accommodated by geometrically necessary dislocations (GNDs), which produce back stress in soft copper domains to make copper domains appear stronger and forward stress in hard iron domains that makes iron domains appear weaker. The interaction between the back stress and forward stress is not a zero-sum game and produces HDI stress to increase the global yield strength of HLS Fe-Cu composites. After the whole HLS sample yields, soft copper domains sustain much higher strain than hard iron domains [7,26,27], producing plastic strain gradients near Fe-Cu domain interfaces. The plastic strain gradients become larger as the strain partitioning increases, producing extra work hardening induced by the hetero-deformation. Based on the Considère criterion, necking starts when the work hardening rate is lower than true flow stress, i.e. $d\sigma/d\varepsilon < \sigma$, where σ is true stress and ε is the true strain. In Fig. 3b, with the extra work hardening, the HLS Fe-Cu composites sustain high strain hardening rate at higher applied strain than pure iron samples, which delays the initiation of necking and thus helps with improving uniform elongation (ductility).

LUR tests were conducted to further probe the impact of synergistic strengthening and HDI hardening on the mechanical performance of HLS Fe-Cu composites. Fig. 4a shows true LUR strain-stress curves of Fe-Cu HLS samples, and the typical hysteresis loops extracted from Fig. 4a are compared in Fig. 4b. Fe-Cu HLS samples with higher volume fractions of copper have wider hysteresis loops, suggesting a stronger Bauschinger effect. HDI stress (σ_{HDI}) is deduced from the hysteresis loops (Fig. 4a) using the method that was used to measure "back stress" [28]:

$$\sigma_{HDI} = \frac{\sigma_u + \sigma_r}{2}, \tag{1}$$

where σ_u is the unloading yield stress, and σ_r is the reloading yield stress. The yield points in unloading and reloading half circles are determined by a plastic strain offset of 5×10^{-4} from the elastic limits. The as-calculated HDI stress is shown in Fig. 4c. The HDI stress increases rapidly at the earlier strain stage and then it slows down with increasing applied strain. The proportion of HDI stress accounts for ~56% of the total flow stress in Fe-15Cu samples and rises to ~65% in Fe-40Cu samples, suggesting that the HDI stress makes major contribution to the high flow strength of HLS Fe-Cu composites and the contribution becomes larger with higher volume fractions of copper. Comparing the HDI hardening (Fig. 4d) with the total strain hardening (Fig. 3b) suggests that the extra strain hardening of HLS Fe-Cu composites during plastic deformation can be mainly attributed to HDI hardening [16,17].

Contributions of both HDI stress and HDI hardening to the mechanical properties of HLS Fe-Cu composites are enhanced with increasing volume fraction of copper. The reason is that adding more copper increases the density of Fe-Cu domain interfaces, producing more areas for GNDs to pile up. It is the GND piling-up that induces HDI strengthening and hardening [16,17,28,29]. As mentioned above, the strength difference between iron and copper domains almost remains the same with varying the density of Fe-Cu domain interfaces. Therefore, it does not affect the synergistic strengthening and HDI hardening in this study.

4. Conclusions

In summary, heterogeneous lamella-structured Fe-Cu composites were produced by powder metallurgy and subsequent thermal-mechanical treatments. Superior mechanical properties of high strength and high ductility were obtained with the heterostructure. It is revealed that the extra strengthening and extra strain hardening are attributed to HDI strengthening and hardening. And their contributions become stronger with increasing the density of Fe-Cu domain interfaces. The density of Fe-Cu domain interfaces was tuned by changing the volume fraction of copper, which has negligible impact on the strength difference between iron and copper domains. This study shows that there is a promising way to produce HLS material with tunable heterostructures by powder metallurgy.

Data availability statement

The raw/processed data required to reproduce these findings cannot be shared at this time as the data also forms part of an ongoing study.

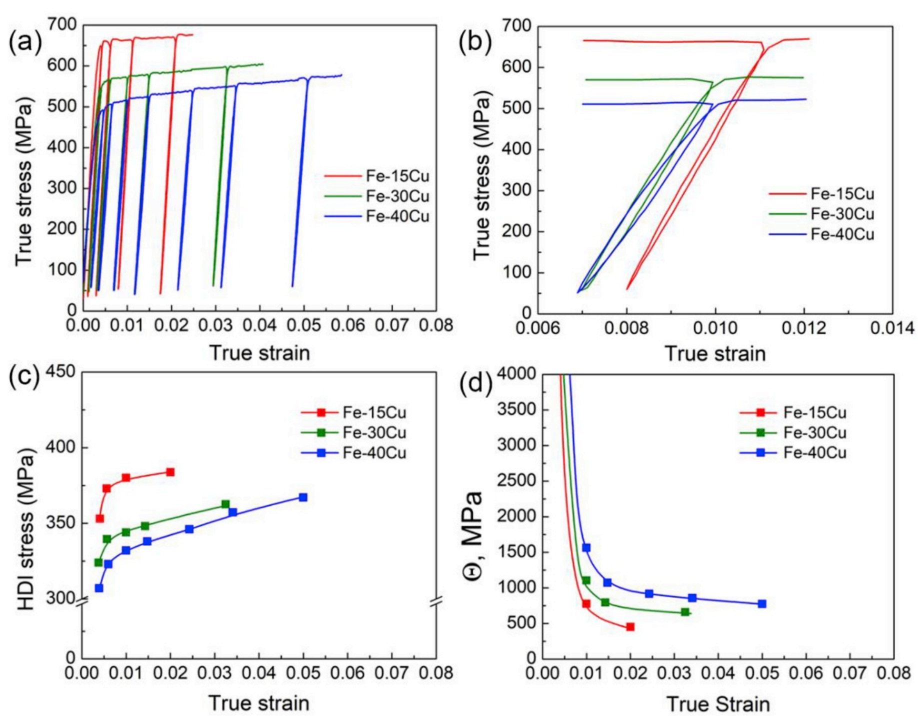

Fig. 4. (a) LUR strain-stress curves of pure homogeneous iron and Fe-Cu HLS samples; (b) Comparison of the hysteresis loops; (c) Comparison of the HDI stress and (d) The HDI hardening rate $\Theta = d\sigma_{HDI}/d\varepsilon_T$ of Fe-Cu samples deduced from Fig. 4a.

Statement of originality

I hereby declare that the research work contained in this thesis is all my original work except where due reference is made.

Declaration of competing interest

The authors declare that they have no known competing financial interests or personal relationships that could have appeared to influence the work reported in this paper.

CRediT authorship contribution statement

Z.K. Li: Conceptualization, Investigation, Methodology, Writing - original draft. **X.T. Fang:** Investigation. **Y.F. Wang:** Investigation. **P. Jiang:** Investigation. **J.J. Wang:** Supervision. **C.M. Liu:** Supervision. **X. L. Wu:** Investigation. **Y.T. Zhu:** Conceptualization, Supervision, Writing - review & editing. **C.C. Koch:** Supervision, Writing - review & editing.

Acknowledgements

This work was supported by the US Army Research Office [W911 NF-12-1-0009]. The authors acknowledge the use of the Analytical Instrumentation Facility (AIF) at North Carolina State University, which is supported by the State of North Carolina and the National Science Foundation. Z.K. Li would like to acknowledge the support from China Scholar Council. Y.T. Zhu was funded by the US Army Research Office.

References

[1] X. Wu, Y. Zhu, Heterogeneous materials: a new class of materials with unprecedented mechanical properties, Materials Research Letters 5 (8) (2017) 527–532.
[2] J. Moering, X. Ma, J. Malkin, M. Yang, Y. Zhu, S. Mathaudhu, Synergetic strengthening far beyond rule of mixtures in gradient structured aluminum rod, Scripta Mater. 122 (2016) 106–109.
[3] C.W. Shao, P. Zhang, Y.K. Zhu, Z.J. Zhang, Y.Z. Tian, Z.F. Zhang, Simultaneous improvement of strength and plasticity: additional work-hardening from gradient microstructure, Acta Mater. 145 (2018) 413–428.
[4] X. Wu, P. Jiang, L. Chen, F. Yuan, Y.T. Zhu, Extraordinary strain hardening by gradient structure, Proc. Natl. Acad. Sci. U. S. A 111 (20) (2014) 7197–7201.
[5] S.K. Vajpai, M. Ota, Z. Zhang, K. Ameyama, Three-dimensionally gradient harmonic structure design: an integrated approach for high performance structural materials, Materials Research Letters 4 (4) (2016) 191–197.
[6] D. Orlov, H. Fujiwara, K. Ameyama, Obtaining copper with harmonic structure for the optimal balance of structure-performance relationship, Mater. Trans. 54 (9) (2013) 1549–1553.
[7] X. Wu, M. Yang, F. Yuan, G. Wu, Y. Wei, X. Huang, Y. Zhu, Heterogeneous lamella structure unites ultrafine-grain strength with coarse-grain ductility, Proc. Natl. Acad. Sci. U. S. A 112 (47) (2015) 14501–14505.
[8] J. Li, Y. Cao, B. Gao, Y. Li, Y. Zhu, Superior strength and ductility of 316L stainless steel with heterogeneous lamella structure, J. Mater. Sci. 53 (14) (2018) 10442–10456.
[9] B.Q. Han, J.Y. Huang, Y.T. Zhu, E.J. Lavernia, Strain rate dependence of properties of cryomilled bimodal 5083 Al alloys, Acta Mater. 54 (11) (2006) 3015–3024.
[10] Y. Wang, M. Chen, F. Zhou, E. Ma, High tensile ductility in a nanostructured metal, Nature 419 (6910) (2002) 912–915.
[11] H. Ghassemi-Armaki, R. Maaß, S.P. Bhat, S. Sriram, J.R. Greer, K.S. Kumar, Deformation response of ferrite and martensite in a dual-phase steel, Acta Mater. 62 (2014) 197–211.
[12] M. Calcagnotto, Y. Adachi, D. Ponge, D. Raabe, Deformation and fracture mechanisms in fine- and ultrafine-grained ferrite/martensite dual-phase steels and the effect of aging, Acta Mater. 59 (2) (2011) 658–670.
[13] X. Ma, C. Huang, J. Moering, M. Ruppert, H.W. Höppel, M. Göken, J. Narayan, Y. Zhu, Mechanical properties of copper/bronze laminates: role of interfaces, Acta Mater. 116 (2016) 43–52.
[14] C.X. Huang, Y.F. Wang, X.L. Ma, S. Yin, H.W. Höppel, M. Göken, X.L. Wu, H.J. Gao, Y.T. Zhu, Interface affected zone for optimal strength and ductility in heterogeneous laminate, Mater. Today 21 (7) (2018) 713–719.
[15] J. Wang, K. Kang, R.F. Zhang, S.J. Zheng, I.J. Beyerlein, J.M. Cabrera, N.A. Mara, Structure and property of interfaces in ARB Cu/Nb laminated composites, JOM (J. Occup. Med.) 64 (10) (2012) 1208–1217.
[16] Y. Zhu, X. Wu, Perspective on hetero-deformation induced (HDI) hardening and back stress, Materials Research Letters 7 (10) (2019) 393–398.
[17] Y.F. Wang, C.X. Huang, X.T. Fang, H.W. Höppel, M. Göken, Y.T. Zhu, Hetero-deformation induced (HDI) hardening does not increase linearly with strain gradient, Scripta Mater. 174 (2020) 19–23.
[18] S. Mula, P. Sahani, S.K. Pratihar, S. Mal, C.C. Koch, Mechanical properties and electrical conductivity of Cu–Cr and Cu–Cr–4% SiC nanocomposites for thermo-electric applications, Mater. Sci. Eng., A 528 (13–14) (2011) 4348–4356.
[19] D. Roy, R. Mitra, O.A. Ojo, S.S. Singh, D. Kolesnikov, W. Lojkowski, R. O. Scattergood, C.C. Koch, I. Manna, Evaluation of mechanical properties of partially amorphous and nanocrystalline Al50Ti40Si10 composites prepared by mechanical alloying and hot isostatic pressing, Mater. Sci. Eng., A 555 (2012) 21–27.
[20] M.D. Demetriou, J.P. Schramm, C. Veazey, W.L. Johnson, J.C. Hanan, N.B. Phelps, High porosity metallic glass foam: a powder metallurgy route, Appl. Phys. Lett. 91 (16) (2007).
[21] P. Yu, K.B. Kim, J. Das, F. Baier, W. Xu, J. Eckert, Fabrication and mechanical properties of Ni–Nb metallic glass particle-reinforced Al-based metal matrix composite, Scripta Mater. 54 (8) (2006) 1445–1450.
[22] R.A. DePaul, A.L. Kitchin, The role of nickel, copper and columbium (niobium) in strengthening a low-carbon ferritic steel, Metallurgical Transactions 1 (1970) 389–393.
[23] C.G. L, K.I.M. Sung-Joon, L.E.E. Tae-Ho, O.H. Chang-Seok, Effects of copper addition on mechanical properties of 0.15C–1.5Mn–1.5Si TRIP-aided multiphase cold-rolled steel sheets, ISIJ Int. 42 (12) (2002) 1452–1456.
[24] M. H, V.Y. Gertsman, H. Gleiter, R. Birringer, The study of grain size dependence of yield stress of copper for a wide grain size range, Acta Metall. Mater. 42 (10) (1994) 3539–3544.
[25] H.S. Kim, Y. Estrin, Ductility of ultrafine grained copper, Appl. Phys. Lett. 79 (25) (2001) 4115–4117.
[26] Z.H. Cong, N. Jia, X. Sun, Y. Ren, J. Almer, Y.D. Wang, Stress and strain partitioning of ferrite and martensite during deformation, Metall. Mater. Trans. 40 (6) (2009) 1383–1387.
[27] C.C. Tasan, M. Diehl, D. Yan, C. Zambaldi, P. Shanthraj, F. Roters, D. Raabe, Integrated experimental–simulation analysis of stress and strain partitioning in multiphase alloys, Acta Mater. 81 (2014) 386–400.
[28] M. Yang, Y. Pan, F. Yuan, Y. Zhu, X. Wu, Back stress strengthening and strain hardening in gradient structure, Materials Research Letters 4 (3) (2016) 145–151.
[29] Y. Lin, J. Pan, H.F. Zhou, H.J. Gao, Y. Li, Mechanical properties and optimal grain size distribution profile of gradient grained nickel, Acta Mater. 153 (2018) 279–289.